Proceedings of PRADS2016
4^{th} – 8^{th} September,2016
Copenhagen, Denmark

Ship motions contribution to the fatigue life of a pre-swirl stator

P.W. Wang [1)], P.K. Liao[1)], C.Y. Hsin[2)], Y. Quéméner[1)] and C.W. Lin[1)]

[1)] Research Department, CR Classification Society, Taipei, Taiwan
[2)] Associate Professor, National Taiwan Ocean University, Keelung, Taiwan

Abstract

This study evaluated the fatigue life of a 5-fin Pre-Swirl Stator (PSS) fitted ahead of the propeller of an 80,000 DWT bulk carrier. Specifically, this study considered the fatigue loads exerted on the fins by the stern wake and the ship motion induced velocity fields, neglecting the effect of the propeller induced inflow. A Boundary Element Method (BEM) based on the potential flow theory was employed to evaluate the loads on the fins. As input for this method, the viscous wake flow was produced by computational fluid dynamic simulations in calm water, and the motion-induced velocity was derived from potential flow based seakeeping analyses. Finally, finite element analyses were carried out using the BEM pressure distribution to extract the hot spot stress at the fin connection, and to thereby assess the fatigue life of the PSS, which was found to be significantly greater than 25 years.

Keywords

Pre-Swirl Stator; Fatigue; BEM; CFD.

Introduction

Since the adoption of the Energy Efficiency Design Index (EEDI) resolution by the IMO (2011), energy efficiency has become a general concern in ship design. Jong (2011) reviewed various existing solutions developed over the past for ship powering improvement. A popular strategy consists of improving the flow into the propeller through the utilization of Energy Saving Devices (ESD) such as Pre-Swirl Stators (PSS). A PSS consists of several stator fins fitted on the stern boss ahead of the propeller. The PSS generates a swirling flow opposite to the propeller rotation that equalizes the propeller inflow and optimizes the propeller efficiency. Although failure of the PSS fins is not critical to the ship's structural integrity, they might impact the propeller after detaching. Therefore, their strength must be carefully considered, especially regarding their fatigue life since cracks were reported as the cause of actual PSS fin failures by Lee and Kim (2015).

Guidelines regarding the direct evaluations of loads for the structural design of PSS are lacking. Yet the PSS fins are subjected to various sources of cyclic loads resulting from ship motions, viscous wake in waves and possibly from Vortex Induced Vibrations (VIV) that jointly contribute to the fatigue. Numerical tools such as Computational Fluid Dynamic (CFD) have been validated by researchers and towing tank facilities to evaluate the benefits of PSS in terms of powering performance. Amongst others, Jong (2011) presented a framework to validate and optimize the Energy Saving Devices (ESD) efficiency using CFD simulations calibrated against model tests. However, CFD analyses are very time consuming and more practical methods are needed to evaluate the loads for structural design. Therefore, researchers have proposed various approaches to address this problem. Paboeuf (2013) proposed a numerical approach to evaluate the structural strength of an ESD for which the design waves producing the maximum bending of the fins would be determined through potential flow based seakeeping analyses, and the corresponding loads exerted on the ESD would be directly analyzed through CFD simulations. Lee and Kim (2015) adopted a similar hybrid potential-viscous flow hydrodynamic computational approach, but a neural network was employed to approximate the CFD-produced hydrodynamic forces as a function of the ship motions thereby enabling rapid long term fatigue predictions.

This study aimed to evaluate the contribution of ship motions to the fatigue life of the PSS fins. Specifically, this study adopted a hybrid potential-viscous flow approach which, compared with CFD, provides a more practical engineering solution for this problem. A Boundary Element Method (BEM) developed by Hsin (1990 & 2003), that is based on the potential flow theory, was used to evaluate rapidly the hydrodynamic loads on the fins for a given regular design wave.

This paper consists of six sections. The first section presents the methodology adopted in this study to assess the PSS fatigue life. The second and third sections describe, respectively, the potential flow based seakeeping analyses and calm water CFD simulations conducted to evaluate the velocity flow field at the PSS. The fourth section presents the BEM fin load predictions. The fifth section compares BEM load predictions to direct CFD simulations in waves. Finally, the sixth section evaluates the fatigue life of the PSS.

Fatigue Life Evaluation Methodology

This study investigated the ship motions effect on the fatigue life of a 5-fin PSS fitted on the stern boss of an 80,000 DWT bulk carrier. Table 1 lists the principal dimensions of the ship. Figure 1 illustrates the PSS fin arrangement for which a number was assigned to each fin.

Table 1: Ship Principal Dimensions

Length between perpendiculars	223 m
Breadth	36.5 m
Draft	13.9 m
Service speed (V_s)	14 knots

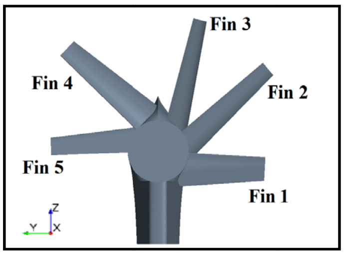

Fig. 1: Pre-Swirl Stator Fin Arrangement

Figure 2 presents the flowchart of the methodology adopted in this study to evaluate the fatigue life of the PSS fins. At first, potential flow based seakeeping analyses were conducted using Hydrostar (BV) to assess the ship motion-induced velocity at the PSS plane for given Equivalent Design Waves (EDW). The EDW approach is a very practical procedure in ship structure design that enables limiting the number of design load cases to the most critical for the structure. For fatigue life assessment, it entails determining the regular waves that generate the loads contributing the most to the fatigue damage that, as established by the IACS (2015b), corresponds to a probability level close to 10^{-2}. Computational Fluid Dynamic (CFD) simulations were then carried out to predict the viscous flow field of the stern wake in calm water.

This study then employed a Boundary Element Method (BEM) developed by Hsin (1990 & 2003) that is based on the potential flow theory to evaluate the PSS fin loads resulting from the unsteady flow field velocity induced by the ship motion and the viscous stern wake as produced by potential flow based seakeeping and calm water CFD analyses respectively. Additionally, this study performed CFD simulations for calm water and in waves for comparison with the BEM fin load predictions.

Afterwards, the pressure distribution produced by the BEM method was transferred onto the finite element model of the fins to extract the hot spot stress range corresponding to the considered EDW. A long term distribution of stress range was then represented by a two-parameter Weibull distribution scaled on the stress range produced for a 10^{-2} probability level and for which the shape factor was set equal to 1.0, according to the IACS (2015a). Finally, the evaluation of the fatigue life for this long term stress range distribution was conducted by using the appropriate S-N curve.

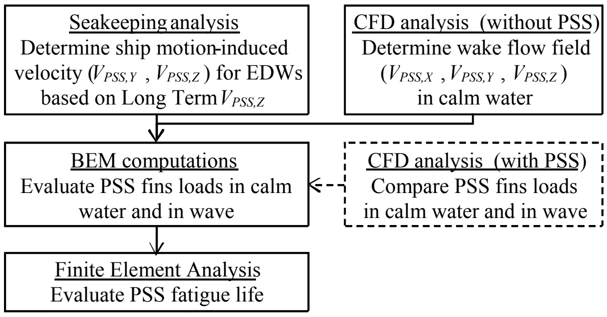

Fig. 2: Flowchart of the Fatigue Life Evaluation Methodology

Equivalent Design Waves for Fatigue Loads

For loads varying linearly with the wave height (e.g. ship hull girder bending moment), the long term value of the load can be directly computed through a spectral analysis conducted on the linear response of the load expressed as a Response Amplitude Operator (RAO). However, the bending moment on the PSS fins would not vary linearly with the wave height, but would relate to the square of the inflow velocity according to the classical drag and lift force formulation for streamlined foil sections. Therefore, this study determined indirectly the EDW maximizing the bending of the fin for the target probability level (P = 10^{-2}) based on the long term value of the ship motion-induced velocity at the PSS, which varies linearly with the wave height, and for which a RAO can thus be produced.

This study adopted the assumptions made by the IACS (2015b) for determining the Rules loads on seagoing ships classed for unrestricted service:

- North Atlantic wave scatter diagram (IACS, 2010),
- Pierson-Moskowitz wave spectrum,
- Angular spreading of the wave energy given by the function cos²,
- 30 deg step of ship/wave heading, and
- Equal heading probability.

The IACS also provides an average speed of 75% the service speed V_s, in addition to which this study assumed an average speed of 100% the service speed.

The seakeeping analyses of the bulk carrier in full load condition were performed in frequency domain using Hydrostar for the two speeds. Figures 3 and 4 show the RAOs of vertical and transverse velocities at the PSS respectively, obtained for various headings at 75%V_s. This study conducted a spectral analysis to produce the long term values of vertical and transverse velocities corresponding to a probability level of 10^{-2}. Table 2 lists the long term values of vertical and transverse velocities for 75%V_s and 100%V_s. It can be observed that the long term vertical velocity was approximately twice the transverse velocity. The vertical velocity would thus have a more significant effect on the cyclic loads exerted on the PSS fins; especially for the horizontal fin No.1 (see Fig. 1) which has the largest projected surface to the vertical velocity action. Additionally, all the fins have an identical scantling. Therefore, fin No.1 was anticipated as being the most critical in view of the fatigue life.

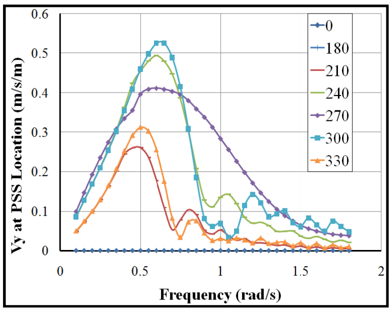

Fig. 3: Transverse Velocity RAOs for 75%Vs

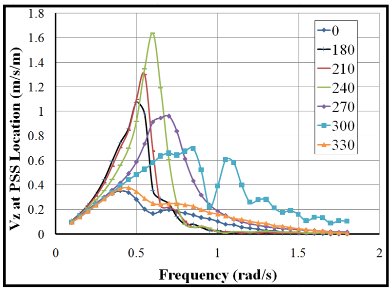

Fig. 4: Vertical Velocity RAOs for 75%Vs

Table 2: Long Term Motion-Induced PSS Velocities

Ship speed	V_y (m/s)	V_z (m/s)
75% V_s	1.21	2.64
100% V_s	1.24	2.88

To ensure that the bending of fin No.1 is maximized, four EDWs were determined for the wave headings with the largest vertical velocity RAO peaks (see Fig. 4): 180 deg (i.e. head sea), 210 deg and 240 deg (i.e. quartering seas), and 270 deg (i.e. beam sea). The head sea EDW only considered the vertical velocity at the PSS generated by the heave and pitch motions, whereas the quartering and beam seas EDWs also included the sway and yaw induced transverse component of the velocity at the PSS.

The four EDWs for head, quartering and beam seas were then derived from the long term value of vertical velocity that would maximize the bending of fin No.1. Equation 1 can compute the EDW amplitude.

$$A_{EDW} = \frac{\text{Long Term } V_{PSS,Z}}{RAO_{max,Vz}} \qquad (1)$$

where $RAO_{max,Vz}$ is the peak of the RAO for the considered heading obtained at the wave frequency ω_{max}.

For the quartering and beam seas EDWs, the additional transverse velocity V_y related to the long term vertical velocity V_z can then be calculated by Eq. 2 which considers the difference in phase between the two velocities V_z and V_y at ω_{max}.

$$V_y = A_{EDW} RAO_{Vy}(\omega_{max}) \times \cos[\Phi_{Vz}(\omega_{max}) - \Phi_{Vy}(\omega_{max})] \qquad (2)$$

where $\Phi_{Vz}(\omega_{max})$ and $\Phi_{Vy}(\omega_{max})$ are the phase angles associated with the EDW wave frequency for the vertical and transverse velocities at the PSS respectively.

Tables 3 and 4 list the equivalent design waves parameters for the two ship speeds 75%V_s and 100%V_s respectively. It can be observed that for a given speed, the vertical component V_z of the velocity was identical for all headings since it is the long term value. However, the largest transverse velocity V_y was obtained for the quartering sea at 240 deg heading. Therefore, the largest bending of the fin could be produced for quartering sea.

Table 3: Equivalent Design Waves for 75%Vs

Heading (deg)	Long-term V_z (m/s)	$RAO_{max,Vz}$ (m/s/m)	ω_{max} (rad/s)	A_{EDW} (m)	V_y (m/s)
180	2.64	1.06	0.50	2.48	0
210	2.64	1.29	0.55	2.05	0.53
240	2.64	1.62	0.60	1.62	0.72
270	2.64	0.96	0.70	2.74	0.69

Table 4: Equivalent Design Waves for 100%Vs

Heading (deg)	Long-term V_z (m/s)	$RAO_{max,Vz}$ (m/s/m)	ω_{max} (rad/s)	A_{EDW} (m)	V_y (m/s)
180	2.88	1.48	0.50	1.94	0
210	2.88	1.49	0.50	1.94	0.37
240	2.88	1.74	0.60	1.66	0.82
270	2.88	0.99	0.70	2.91	0.75

Wake Velocity Field by Calm Water CFD

This study performed CFD computations of the ship in calm water using Star-CCM+ (CD-Adapco, 2015). However, the CFD simulations were conducted omitting the PSS geometry in order to extract the nominal stern wake velocity flow field in the PSS region. Therefore, the CFD simulation represented only the starboard side of the hull using the ship symmetry. Trimmer mesh was then provided for the entire domain and refined meshing was added near the free surface region for more accurate wave patterns. Figure 5 shows the computational domain extent and meshing strategies. A Finite Volume Method was adopted to discretize the computational domain and to calculate the Reynolds-Averaged Navier-Stokes (RANS) equations with the suitable turbulence model. Finally, the free surface was modeled through the Volume-of-Fluid (VOF) approach.

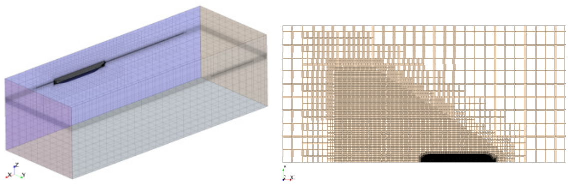

Fig. 5: CFD Computational Domain Extent and Meshing

This study conducted calm water CFD analyses allowing two degrees of freedom (i.e. sinkage and trim) for two speeds (i.e. 75%V_s and 100%V_s) and comprising 2,350,000 cells. Figure 6 shows the three longitudinal locations from the leading to the trailing edges of the PSS fins (left) and the radial positions (right) covering the PSS region at which the nominal wake velocity flow field (V_x, V_y, V_z) was extracted from the CFD calculations. Figure 7 presents the wake velocity flow field evaluations obtained by CFD for 75%V_s. It can be observed from the velocity contours that the axial velocity component V_x at the PSS was much reduced by the stern geometry, while the vector plot, showing the vertical and transverse components of the velocity, illustrate the vorticity present at the PSS plane.

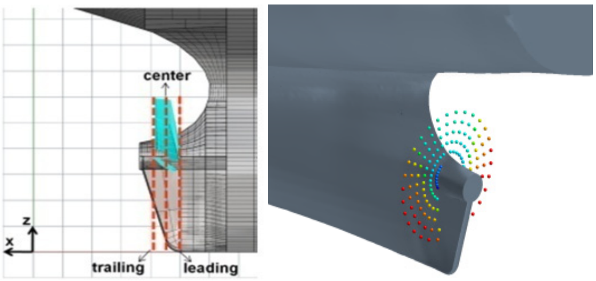

Fig. 6: Region of the Nominal Wake Flow Field

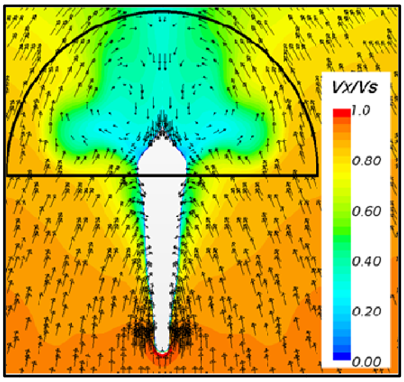

Fig. 7: Stern Wake Velocity Field at the PSS for 75%V_s

PSS Fin Load Evaluations by BEM

This study evaluated the fatigue loads exerted on the PSS fins by employing a Boundary Element Method (BEM) developed by Hsin (1990 & 2003) that is a perturbation potential based boundary element method, and for which the governing equation is provided in Eq. 3, with the coordinate system fixed on the PSS.

$$2\pi\phi_p(t) = \int_{S_P}[\phi(t)\frac{\partial G}{\partial n} - G\frac{\partial \phi}{\partial n}(t)]dS + \int_{S_W}\Delta\phi(\vec{x},t)\frac{\partial G}{\partial n}dS] \quad (3)$$

where S_P denotes the PSS fin surface, and S_W denotes the PSS fin wake surface. G is the Green function and n is the normal vector. The Green function G can also be explained as the potential induced by a unit strength source, and $\partial G/\partial n$ can be explained as the potential induced by a unit strength dipole. $\phi(t)$ is the strength of perturbation potentials, equivalent to the dipole strength. $\partial\phi/\partial n$ is the source strength, and it can be determined by the boundary condition given in Eq. 4.

$$\frac{\partial\phi}{\partial n}(t) = -\vec{U}_{in}(\vec{x},t).\vec{n} \quad (4)$$

where $\vec{U}_{in}(\vec{x},t)$ is the inflow velocity relative to the PSS blades, and is a function of position and time, and $\Delta\phi$ is the dipole strength in the wake, which, from the Kutta condition, is the difference between the dipole strengths at upper and lower trailing edge panels.The source strength in the wake is zero since the wake has zero thickness.

The discretized form of Eq. 3 is formulated in Eq. 5.

$$\sum_{k=1}^{N_B}\left[\sum_{j=1}^{N_P(k)} a_{i(k),j(k)}\mu^n_{j(k)} + \sum_{m=1}^{M(k)} W_{i(k),m(k),l(k)}\Delta\phi^n_{m(k),l(k)}\right] = RHS^n_{i(k)}$$

$$i(k) = 1, N_P(k); \quad k = 1, N_B \quad (5)$$

$$RHS^n_{i(k)} = \sum_{k=1}^{N_B}\left[\sum_{j=1}^{N_P(k)} b_{i(k),j(k)}\sigma^n_{j(k)} - \sum_{m=1}^{M(k)}\sum_{l=2}^{N_W(k)} W_{i(k),m(k),l(k)}\Delta\phi^n_{m(k),l(k)}\right]$$

where N_B is the number of PSS fins, and for PSS fin k, $N(k)$ is number of panels chord-wise, $M(k)$ is number of panels span-wise, and $N_P(k)$ is total number of panels, $N_P(k)$=$N(k)$*$M(k)$. $N_W(k)$ is number of panels chord-wise in the wake. μ_j and σ_j represent the discrete forms of ϕ and $\partial\phi/\partial n$, $a_{i,j}$, $b_{i,j}$ represent the discrete forms of the integrations of $\partial G/\partial n$ and $1/r$ over a panel, and r is the distance between the panel point and the induced point p. $a_{i,j}$ and $b_{i,j}$ are defined as the "influence functions" of the dipoles and sources respectively from panel j to collocation point i. W represents the discrete forms of the integration of $\partial G/\partial n$ over a wake panel. The superscript n denotes the time step (relative to the incoming wave), and time t is defined as $t = n\Delta t$. A time marching numerical scheme is adopted for the solution, and the inflow velocity is updated at each time step.

The velocity flow field around the PSS (V_x, V_y, V_z) consists of three components: the ship stern wake, the ship motion-induced velocity at the PSS and the wave particle velocity. This study neglected the effect of the wave particle velocity that is vanishing with the distance to the sea surface. For the considered EDWs, the minimum waterhead above the PSS was approximately 8 m which is considered deeply submerged. Additionally, the stern wake and the ship motions contributions to the velocity flow field were linearly combined, assuming that their effects were independent and that the stern wake flow field remained unchanged in waves.

The viscous stern wake flow field (V_x, V_y, V_z) and the cyclic motion-induced velocity flow field (V_y, V_z) were input into the BEM to compute the loads exerted on the PSS fins. Figure 8 shows a typical fin panel model employed for the BEM calculations.

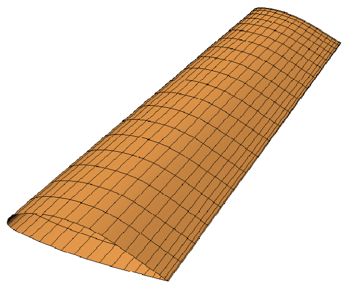

Fig. 8. Fin Model for BEM Computations

Figures 9 to 11 show the BEM predictions of the three directions of force (F_x, F_y, F_z) exerted over each fin for the two following cases:

- Calm water at 75%V_s (dash line), and
- Head sea (see Table 3, 180deg) at 75%V_s (full line).

It can be observed that amongst all the force components, the vertical force (F_z) produced the largest range of loads, especially on fin No.1, which was subjected to the largest range of vertical forces. Therefore, the BEM force prediction confirmed the criticality in view of the fatigue of fin No.1, as previously anticipated when determining the EDWs based on the long term value of the vertical velocity at the PSS. Additionally, because of the pitch angle of fin No.1, the axial component of the force (F_x) might also have a significant influence on the fin bending.

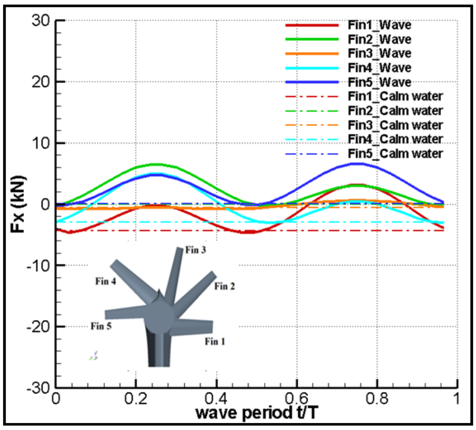

Fig. 9: PSS F_x Prediction by BEM for 75%Vs

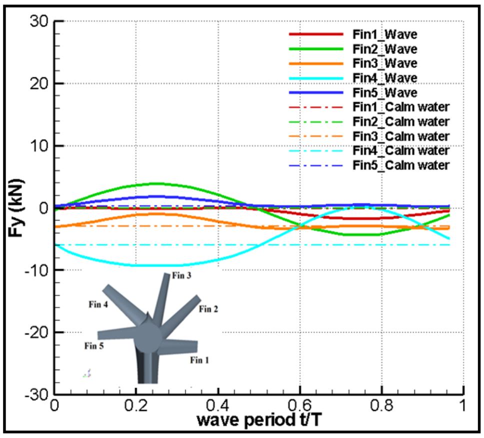

Fig. 10: PSS F_y Prediction by BEM for 75%Vs

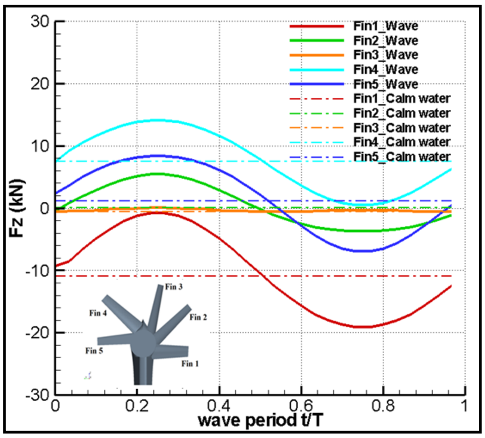

Fig. 11: PSS F_z Prediction by BEM for 75%Vs

Figure 12 shows the BEM prediction of bending moment about fin No.1's chord axis for the four EDWs (i.e. Headings = 180 deg, 210 deg, 240 deg and 270 deg) and two speeds (i.e. 75%V_s and 100%V_s).

It can be observed that for each speed, the BEM predictions were similar for the four EDWs. Table 5 lists the range of bending moments exerted at fin No.1 produced by each EDW. It appeared that for the two speeds, the quartering sea EDW with a heading of 240 deg resulted in a bending moment range approximately 23% larger than that obtained for the head sea EDW. Finally, for the quartering sea EDW with a heading of 240 deg, the 100%V_s speed generated a bending moment approximately 40% larger than that obtained for the 75%V_s speed. Therefore, it was anticipated that the highest hot spot stress range and thus the lowest fatigue life would be produced for the quartering sea EDW with a heading of 240 deg at 100%V_s speed.

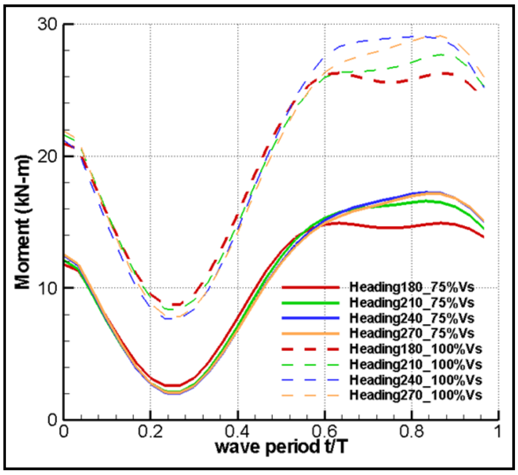

Fig. 12: Fin No. 1 Bending Moment Prediction by BEM

Table 5: Fin No.1 Bending Moment Range (kN.m) by BEM

Heading (deg)	**Ship speed** **75%V_s**	**100%V_s**
180	12.32	17.53
210	14.44	19.33
<u>240</u>	<u>15.26</u>	<u>21.42</u>
270	15.10	21.28

Comparison of the BEM and CFD Evaluations

This study conducted three CFD analyses for comparison with the BEM predictions:

- Calm water for 75%V_s,
- Calm water for 100%V_s, and
- EDW head sea for 75%V_s (see Table 3, 180 deg).

The CFD settings were the same as presented previously to determine the wake flow field in calm water condition, except that, because of the asymmetric arrangement of the PSS fins (see Fig. 1), the two sides of the ship were represented, resulting in a mesh of 5,620,000 cells.

Fin Loads Prediction in Calm Water

Figures 13 to 15 show each component of the hydrodynamic force exerted on each fin determined by BEM and CFD computations in calm water for the two speeds. Some deviations can be observed between the BEM and CFD results for each speed assumption. However, the trends obtained by BEM and CFD analyses were similar, especially, for fin No.1, where the F_x CFD prediction was approximately 25% larger than the BEM results, and the F_y and F_z evaluations by both approaches were very similar. Therefore, for fin No.1, the BEM results were in good agreement with the CFD predictions in calm water.

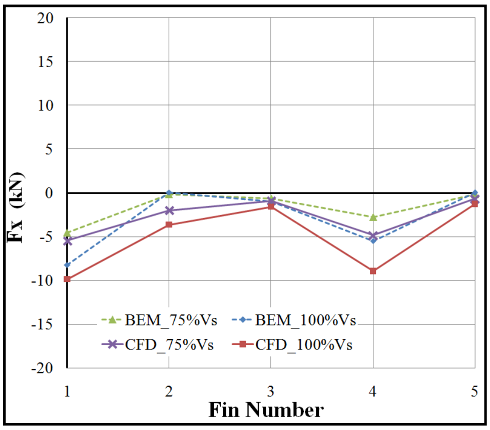

Fig. 13: PSS F_x Prediction by BEM and CFD in Calm Water

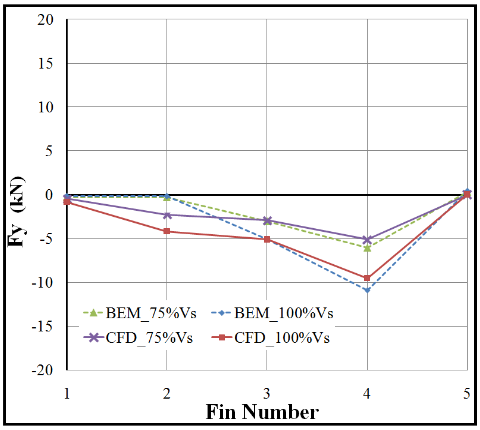

Fig. 14: PSS F_y Prediction by BEM and Calm Water CFD

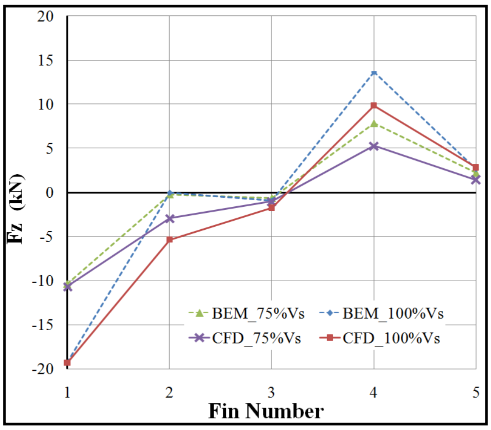

Fig. 15: PSS F_z Prediction by BEM and Calm Water CFD

Figure 16 shows the velocity field around fin No.1 obtained by CFD analyses at three section planes taken along the length of fin No.1. In the r_1-plane, it can be observed that the fluid separated from the leeward surface probably due to a large attack angle. However, the BEM methods based on potential theory cannot consider this effect of separation. Although the separation tended to disappear for the planes r_2 and r_3, the separation close to the root can explain the load deviations between the BEM and CFD analyses. Furthermore, fins No. 2, 3 and 4, are in low inflow velocity areas (see Fig.7) which might increase the angles of attack and generate more flow separation that cannot be properly handled by the BEM and could thus explain the larger deviations observed between BEM and CFD results.

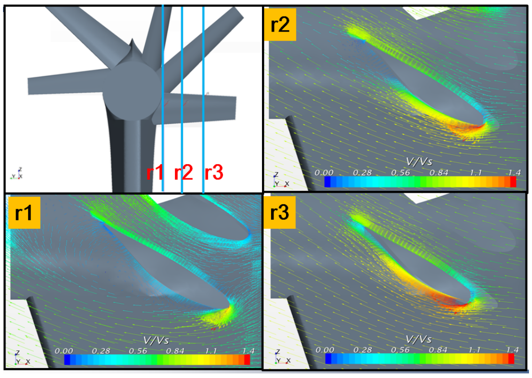

Fig. 16: Velocity Flow Field at fin No.1 by CFD

Fin Loads Prediction in Regular Waves

This study performed CFD simulations including the pitch and heave motions of the ship in head sea at $75\%V_s$ considering a regular equivalent design wave of 4.96 m height and 12.6 s period (see Table 3, 180 deg). Figure 17 presents the wave pattern obtained by CFD. Table 6 lists the heave and pitch motions obtained through CFD analyses and those produced by the potential flow (PF) based seakeeping analyses. A slight wave dissipation appeared during the CFD simulations with a wave height at the bow of 4.85 m. Additionally, in Table 6, it can be observed that the CFD heave motion amplitude was approximately 13% lower than that obtained by potential flow (PF) based seakeeping analyses, whereas the pitch response produced by both analyses were similar. The ship motions obtained by CFD were thus in good agreement with the potential flow (PF) based seakeeping predictions.

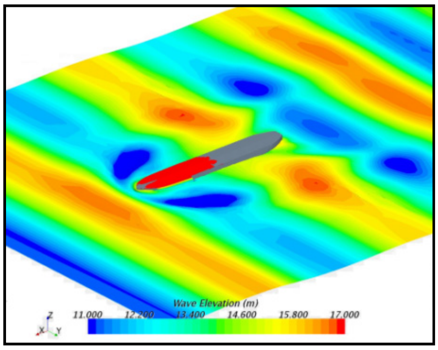

Fig. 17: Wave Pattern and Ship Motions by CFD Analyses

Table 6: Heave and Pitch Motions Amplitude Prediction by CFD and PF Seakeeping Analyses

Analysis Types	Heave (m)	Pitch (deg)
CFD	2.13	2.36
PF Seakeeping	2.44	2.40

Figure 18 shows the vertical forces exerted on fin No.1 obtained by BEM and CFD calculations in waves. It can be observed that as the ship was pitching bow up (t = 158 s and 168 s), the CFD prediction was slightly smaller than the BEM results, whereas as the ship was pitching bow down (t = 164 s), the deviation was much larger. Fluid separation induced by an extensive attack angle may explain this load overestimation by the BEM which cannot reproduce the viscous flow effect.

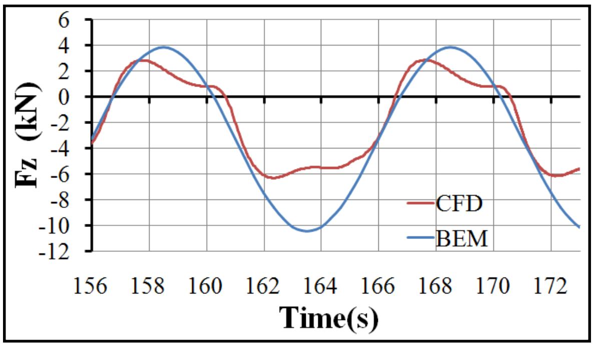

Fig. 18: Fin No.1 F_z Predictions in Wave by BEM and CFD

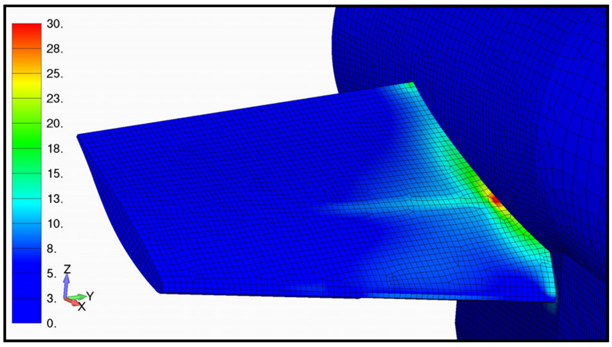

Fig. 20: Principal stress contour on the PSS FE model

Figure 19 shows the bending moment about the chord axis of the fin No. 1, obtained by BEM and CFD calculation in waves. It appeared that the results obtained by both approaches had a very similar cyclic trend, but also a significant shift of the mean value. However, bending moment ranges of 12 kN.m and 10 kN.m can be observed for the BEM and CFD computations respectively, leading to a 20% BEM overestimation compared to the CFD results. Therefore, the cyclic range of bending moment was in good agreement between both approaches. The BEM approach would thus produce a slightly conservative load prediction for fatigue assessment, since the fatigue life would mostly be related to the range of bending moment.

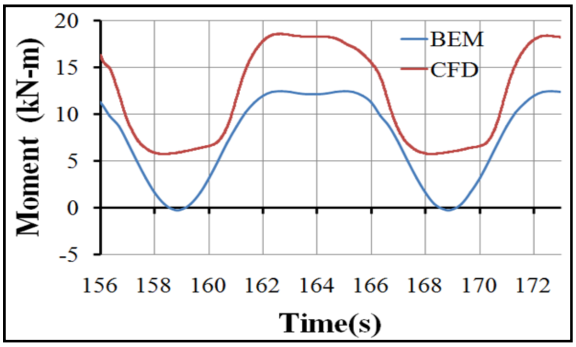

Fig. 19: Fin No.1 Bending Moment Prediction in Wave by BEM and CFD

Structural Fatigue Life Evaluation

This study carried out static Finite Element Analyses to evaluate the PSS fin No.1 structure response, especially to extract the maximum hot spot stress range at the fin connection to the stern boss structure. Figure 20 shows the FE model of the PSS including fin No.1 and the stern boss structure. The FE model was made of 'Shell' elements with a very fine mesh size corresponding to the element thickness at the fin connection where the hot spot stress was extracted.

The fore end of the stern boss FE model was set as fixed. The pressure distribution over fin No.1 produced by the BEM computations was transferred onto the fin FE model. Additionally, the cyclic hydrostatic pressure was applied onto the fin as it related to the ship motion-induced waterhead at the PSS that varied approximately between 8 m and 12.5 m for all the examined EDWs. Finally, gravity was included as a vertical downward acceleration of 9.81 m/s^2.

The largest hot spot stress range was then extracted from the highly stressed element in Fig.20, and the corresponding two-parameter Weibull long term stress range distribution was scaled on this reference stress range obtained for a probability level of 10^{-2}, as described in the methodology. The fatigue life was then assessed using the S-N curve provided by the IACS (2015a) for a total number of cycles of approximately 7.1×10^7 over the 25 years of the ship life calculated by Eq. 6, provided by the IACS (2015a).

$$N_D = 31.557 \times 10^6 \left(f_0 T_D\right) / 4 \log L \qquad (6)$$

where f_0 is the percentage of life time in operation set as 85%, T_D is the design life taken as 25 years and L is the ship length.

Table 7 presents the results of the fatigue life evaluations. It can be observed that for 75%V_s and 100%V_s, the lowest fatigue life was obtained for a wave heading of 240 deg with the associated predicted fatigue lives (T_F) of 2575 years and 518 years respectively. Therefore, the fatigue strength of the pre-swirl stator examined in this study was found satisfactory, although the fin hydrodynamic bending moment range produced by BEM was slightly more conservative than that of the CFD calculations (see Fig. 19). Additionally, the average speed assumption had a significant effect on the fatigue life prediction, since a speed increase of 33% resulted in an 80% reduction in predicted fatigue life.

Table 7: Fatigue Life Evaluations Detailed Results

Heading (deg)	**Ship speed**					
	75%V_s			**100%V_s**		
	$\Delta\sigma_{HS}$ (N/mm^2)	D (-)	T_F (year)	$\Delta\sigma_{HS}$ (N/mm^2)	D (-)	T_F (year)
180	22	0.005	4848	30	0.021	1180
210	25	0.009	2637	32	0.031	808
<u>240</u>	<u>25</u>	<u>0.010</u>	<u>2575</u>	<u>36</u>	<u>0.048</u>	<u>518</u>
270	24	0.007	3465	33	0.037	679

Conclusions

This study evaluated the fatigue life of a pre-swirl stator fitted on the stern boss ahead of the propeller. Specifically, this study evaluated the ship motions contribution to the fatigue life of the PSS fins. This study adopted a hybrid potential-viscous flow approach which, compared with CFD, provides a more practical engineering solution for this problem. A Boundary Element Method

(BEM) developed by Hsin (1990 & 2003), that is based on the potential flow theory, was used to evaluate rapidly the hydrodynamic loads on the fins for a given regular design wave. Calm water CFD simulations were conducted to evaluate the viscous stern wake's nominal velocity field. Potential flow based seakeeping analyses were carried out to produce the motion-induced velocity at the PSS for various Equivalent Design Waves (EDW). The EDWs were defined based on the long term predictions of vertical velocity at the PSS for head, quartering and beam sea headings, and for two ship speeds set as 75% and 100% the service speed. The BEM predicted that the horizontal fin No.1 was subjected to the largest bending loads.

The advantage of the BEM was that it did not require conducting very time consuming CFD simulations in waves. However, this method relied on several assumptions that need to be further validated. Therefore, CFD simulations in waves were conducted for comparison with the BEM results. First, it appeared that the load predictions in calm water were in good agreement for both approaches, especially for fin No.1. On the other hand, the observation of the fin No.1 bending moment in waves shows that the BEM predictions were significantly shifted down compare to the CFD results, but the range value was only 20% higher than that produced by CFD which would thus lead to a reasonably conservative fatigue life estimate. The BEM approach is thus a convenient approach allowing for rapid fin load evaluation with reasonable accuracy. However, the comparison with CFD enabled the authors to also identify the local flow separation on the leeward side of the fin. In the future, the consideration of the propeller inflow velocity in calm water by CFD would reduce the attack angle and thus limit the influence of separation on the fin load predictions. A limiting pressure to the potential flow prediction for attack angle exceeding the stall angle would also enable reducing the BEM overestimations. Finally, the BEM calculations were conducted assuming that the stern wake flow field produced by CFD in calm water remained unchanged in waves. This enabled the authors to avoid carrying out time expensive CFD simulations in waves. However, additional CFD simulations in waves omitting the PSS geometry would be necessary to observe variations of the nominal wake flow field in order to validate this assumption.

Finally, this study carried out finite element analyses of the PSS structure using the BEM pressure distribution combined with the cyclic hydrostatic waterhead pressure and gravity. The maximum hot spot stress range extracted at the fin No.1 connection to the stern boss was produced for the EDW of 240 deg wave heading (i.e. quartering sea) and the evaluated fatigue lives were of 2575 years and 518 years for 75% and 100% service speed respectively. Therefore, the PSS fatigue strength was found satisfactory even though the BEM loads were found to be conservative compared to the CFD prediction. The average speed assumption had also a significant effect on the fatigue life evaluation.

References

CD-Adapco (2015), Star-CCM+ User Guide

Hsin (1990), "Development and Analysis of Panel Methods for Propellers in Unsteady Flow" ,PhD thesis, Department of Ocean Engineering, M.I.T.

Hsin(2003), "Development of a Boundary Element Method to the Computations of Flow Around POD Propulsion Systems", Journal of Taiwan Society of Naval Architects and

IACS, (2015a), "Harmonized Common Structural Rules for Bulk Carriers and Oil Tankers", IACS, London.

IACS, (2015b), "Technical Background Reports for the Harmonized Common Structural Rules for Bulk Carriers and Oil Tankers" No.5, IACS, London.

IACS, (2001). ‘Standard Wave Data’. Recommendation (Rec.) No.34, IACS, London.

IMO, (2011). "Inclusion of regulations on energy efficiency for ships in MARPOL Annex VI", MEPC.203(62)

de Jong, JH (2011). "A Framework for Energy Saving Device (ESD) Decision Making", Proc. International Conference on Ship Efficiency, Hamburg.

Lee, DB, and Kim, HJ (2015). "A Study on the Short and Long-term Analysis of Nonlinear Hydrodynamic Force on an Energy Saving Device", Analysis and Design of Marine Structures, Taylor & Francis, London, UK, pp713-721.

Paboeuf (2013), "ESDs Structural Assessment", RETROFIT &GRIP Midterm Conference, Rotterdam, The Netherlands.